Chemical Mapping of Semiconductor Interfaces at Near-Atomic Resolution

A. Ourmazd, D. W. Taylor, and J. Cunningham
AT&T Bell Laboratories, Holmdel, New Jersey 07733

C. W. Tu
AT&T Bell Laboratories, Murray Hill, New Jersey 07974
(Received 15 July 1988)

We combine chemical lattice imaging with digital pattern recognition to map, at near-atomic resolution, the compositional change across GaAs/AlGaAs interfaces of the highest optical quality. These maps quantify the information content of each unit cell of the lattice image. Our results show that state-of-the-art GaAs/AlGaAs interfaces contain substantial atomic roughness on scales finer than suggested by optical measurements.

PACS numbers: 68.55.Nq, 61.16.Di, 68.35.Dv, 68.65.+g

The fascinating optical and electronic properties of modern multilayered systems are strongly influenced by the structure of their heterointerfaces, which have been much investigated.[1-8] In all but the most heavily mismatched compound semiconductor systems, the atoms occupy zinc-blende sites at and on both sides of the interface. Interfacial roughness is a few monolayers, with one monolayer being the most commonly quoted value. Interruption of growth before the deposition of a succeeding layer reduces interfacial roughness. The lateral spacing between interfacial steps, deduced from optical measurements, appears to be of the order of microns. However, the quantitative determination of the lattice site occupancy at and around an interface, and the correlation of this information with the optical and electronic properties of the same interface remain important experimental and theoretical challenges.

The determination of the site occupancy at a semiconductor heterointerface, and hence the interfacial atomic configuration requires chemical information on an atomic scale. In this Letter, we combine the recently developed chemical imaging technique[9] with digital pattern recognition to determine the atomic configuration of two sets of optically well-characterized, high-quality GaAs/$Al_{0.37}Ga_{0.63}As$ interfaces, grown with and without interruption. In images of cross-sectional samples ~ 75 Å thick, we determine the composition of individual unit cells 2.8×2.8 Å^2 in area, and give confidence levels for the accuracy of our determination at each cell in the lattice image. Our analyzed lattice images map the sample composition at near-atomic resolution, both chemically and spatially. Such maps establish that interfaces of the highest optical quality are not atomically smooth, and that the spacing between interfacial steps, i.e., the island sizes are smaller than previously thought.

The interrupted growth samples were produced by standard molecular-beam epitaxy (MBE) with growth interruption of 2 min at each interface, as reported elsewhere.[10] The samples grown without interruption were produced by gas-source MBE. All samples displayed "monolayer" splitting of the photoluminescence lines, with linewidths among the smallest currently achieved, and represent the state of the art.[10] Chemical lattice images were obtained in a ⟨100⟩ cross section with a JEOL 4000EX high-resolution transmission electron microscope operating at 400 keV, with sample thicknesses (~ 75 Å) and lens defocus values (~ -200 Å) corresponding to maximum chemical sensitivity.[9]

Figure 1 is a typical chemical lattice image of a GaAs/$Al_{0.37}Ga_{0.63}As$ heterostructure grown with interruption. Briefly, the chemical lattice-imaging technique utilizes the bandpass characteristics of the microscope objective lens to enhance the transmission of the chemically sensitive (200) reflections in the ⟨100⟩ projection, thus producing a large change in the spatial frequency content of the lattice image as the interface is crossed. The chemical information is encoded in the patterns that GaAs and AlGaAs produce. Thus, the GaAs lattice-image unit-cell pattern consists of five white blobs, placed at the four corners and the center of a square,

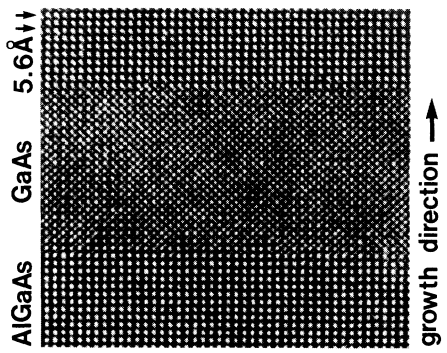

FIG. 1. Chemical lattice image of a GaAs/$Al_{0.37}Ga_{0.63}As$ quantum well produced after 2-min growth interruption at each interface. Careful inspection reveals interfacial regions have images intermediate between GaAs and $Al_{0.37}Ga_{0.63}As$.

while the $Al_{0.37}Ga_{0.63}As$ pattern consists only of four large white blobs at the corners of a similar square [Fig. 2(a)].

Lattice images such as Fig. 1 are traditionally evaluated by simple visual inspection. This is not sufficient for our purpose of determining the composition at each lattice-image unit cell. It is necessary to determine the way that random variations due to surface damage, contamination, and shot noise cause uncertainty in the evaluation of lattice images. Briefly, this is achieved as follows.[11] First, we obtain an "ideal," noise-free image of the projected unit cell for each of the two materials by averaging over many lattice-image unit cells not at the interface. The resulting images act as templates for the recognition of GaAs and $Al_{0.37}Ga_{0.63}As$ [Fig. 2(a)]. Each template is divided into a 35×35 pixel array, and the intensity in each pixel is recorded. We define a vector $\mathbf{R}^t$, whose components are the intensity values at each pixel of the template. Thus the ideal GaAs and AlGaAs unit cells are each represented by a 1225-component vector template. The change in composition from GaAs to AlGaAs can now be defined in terms of the angle θ_c between these two vectors [Fig. 2(b)]. We represent a given unit cell of the real (i.e., noisy) image also by a vector $\mathbf{R}$. For "bulk" GaAs not at the interface, the vectors $\mathbf{R}_{GaAs}$ representing the lattice-image unit cells form a distribution about $\mathbf{R}^t_{GaAs}$, with the angles between $\mathbf{R}^t_{GaAs}$ and $\mathbf{R}_{GaAs}$ representing the effect of noise. The standard deviation σ of this distribution quantifies the noise present in the image of GaAs [Fig. 2(c)]. A similar procedure is used to quantify the noise in "bulk" AlGaAs. The noise present is such that $\mathbf{R}_{GaAs}$ and $\mathbf{R}_{AlGaAs}$ form similar normal distributions about their templates, with the template vectors $\mathbf{R}^t_{GaAs}$ and $\mathbf{R}^t_{AlGaAs}$ about 12σ apart. This means that as the Al concentration is increased from 0 to 0.37, the template vector $\mathbf{R}^t$ rotates through an angle which is 12σ. Thus, our vector representation of the lattice image allows us to distinguish between GaAs and $Al_{0.37}Ga_{0.63}As$ with total confidence.

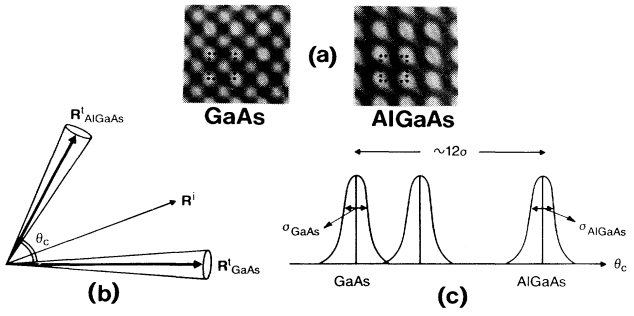

FIG. 2. (a) Averaged, noise-free images of GaAs and $Al_{0.37}Ga_{0.63}As$. The unit cells used as templates for pattern recognition are the dotted 2.8-Å squares. (b) Schematic representations of the template vectors $\mathbf{R}^t_{GaAs}$ and $\mathbf{R}^t_{AlGaAs}$, the distribution of $\mathbf{R}_{GaAs}$ and $\mathbf{R}_{AlGaAs}$ about them, and an interfacial vector $\mathbf{R}^i$. (c) Schematic representation of the distributions produced by the GaAs and $Al_{0.37}Ga_{0.63}As$ unit cells about their templates. Note that the angular position of $\mathbf{R}^i$ denotes the most likely composition only. The actual composition falls within a normal distribution about this point.

We next consider vectors $\mathbf{R}^i$ representing the image unit cells in the close vicinity of the interface. Our image simulations and control experiments show that the projection of $\mathbf{R}^i$ onto the plane defined by the template vectors rotates monotonically and linearly between the two template vectors as the Al content is changed. Thus the angular position of $\mathbf{R}^i$ with respect to the template vectors $\mathbf{R}^t_{GaAs}$ and $\mathbf{R}^t_{AlGaAs}$ yields the Al content of the 2.8×2.8-Å^2 unit cell. At all the interfaces we have analyzed, a substantial number of vectors $\mathbf{R}^i$ fall more than 3σ away from both the template vectors $\mathbf{R}^t_{GaAs}$ and $\mathbf{R}^t_{AlGaAs}$. Assuming the noise content of the image to be the same at and in the vicinity of the interface, such vectors represent, with a confidence of at least 3 parts in 10^3, unit cells of $Al_xGa_{1-x}As$, with $0<x<0.37$. The actual composition of the unit cell represented by a vector $\mathbf{R}^i$ must fall within $\sim3\sigma$ of the value deduced from the angular position of $\mathbf{R}^i$. Thus, the approach we have outlined allows the determination of the Al content of individual interfacial unit cells $2.8\times2.8\times75$ Å^3 in size. A unit cell *at* an atomically abrupt interface is composed of $\frac{1}{4}$ $Al_{0.37}Ga_{0.63}As$ and $\frac{3}{4}$ GaAs or vice versa, depending on the choice of origin. Thus an abrupt interface would be characterized by a transition from GaAs to $Al_{0.37}Ga_{0.63}As$ via a single unit cell, with an Al content of $\frac{1}{4}\times0.37$ or $\frac{3}{4}\times0.37$, depending on the unit-cell position adopted.

Figure 3 is a possible representation of a chemical lattice image analyzed as described above, where the individual lattice-image unit cells are placed at different heights. The height of a unit cell represents the angular position of its vector $\mathbf{R}$ with respect to the template vectors. The height can thus be interpreted in terms of the Al concentration, going from 0 to 0.37 from the bottom to the top of the three-dimensional representation.[12] The blue and yellow regions indicate those unit cells falling within 3σ of $Al_{0.37}Ga_{0.63}As$ and GaAs, respectively, while the other colors break up the data into a different standard deviation, or composition bands. This representation allows a quantitative display of the noise in the GaAs and AlGaAs regions, and the change in the angular position of $\mathbf{R}$ with respect to the templates on crossing the interface. It thus provides a spatial map of the composition, at near-atomic resolution. With our choice of unit-cell origin, an atomically abrupt interface would result in a transition from GaAs to AlGaAs via a single (green) interfacial unit cell at a height $\frac{1}{4}$ that of a blue $Al_{0.37}Ga_{0.63}As$ unit cell. It is clear that this is not realized, and that the interface is not smooth.[13] Figure 3, which is typical, shows that the transition from GaAs to

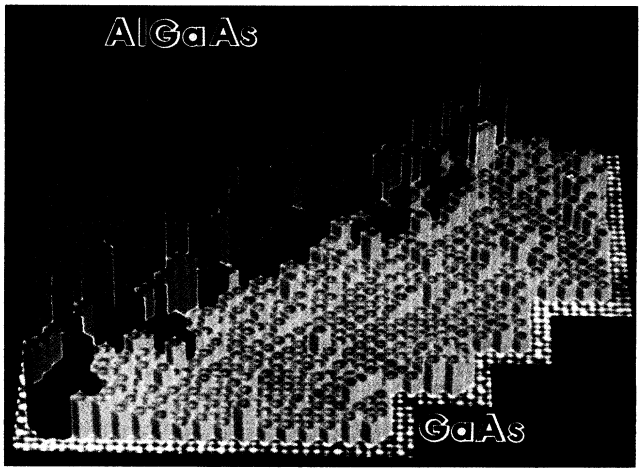

FIG. 3. Three-dimensional representation of the analyzed lattice image of $Al_{0.37}Ga_{0.63}As$ grown on GaAs after a 2-min interruption. The unit cells are 2.8-Å squares. The height of each cell represents the angular position of its vector **R** with respect to the template vectors, which are about 12σ apart. Yellow and blue mark those cells which fall within 3σ of GaAs and $Al_{0.37}Ga_{0.63}As$ templates, respectively. Green, magenta, and red represent 3σ bands centered about 3σ, 6σ, and 9σ points from GaAs. Outside the yellow and blue regions, the Al content of each unit cell is intermediate between GaAs and $Al_{0.37}Ga_{0.63}As$, with confidence levels given by normal statistics.

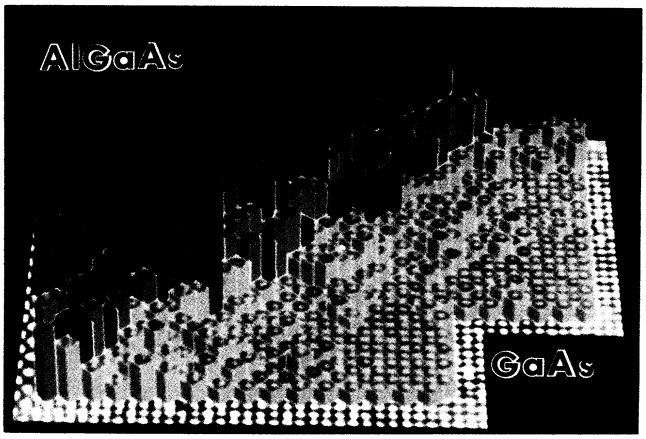

FIG. 4. Three-dimensional representation of the analyzed chemical image of $Al_{0.37}Ga_{0.63}As$ grown on GaAs without interruption. Color-coding and unit-cell size are the same as Fig. 3. Note the presence of small, disjointed clusters of color, indicating finer scale roughness.

$Al_{0.37}Ga_{0.63}As$ takes place over 2–4 unit cells, and that the interface contains significant atomic roughness. At the level of detail of our composition maps, the assignment of values for interfacial imperfections, such as transition width, roughness, and island size, is a matter of definition. Also, without extensive sampling caution is required in deducing quantitative values for the spacing between interfacial steps, however, they are defined. Nevertheless, it is clear that significant atomic roughness at the ~50-Å lateral scale is present. Figure 4 shows the analyzed chemical lattice image of a GaAs/$Al_{0.37}Ga_{0.63}As$ interface produced without growth interruption. Increased interfacial roughness is now apparent in that no single color band can be continuously followed along the interface for more than a few unit cells.[14]

A detailed discussion of the effect of growth parameters on interfacial roughness will be published elsewhere. However, our results already show that samples of the highest optical quality, grown with or without interruption, can exhibit significant interfacial roughness on an atomic scale. Interrupted-growth MBE interfaces are somewhat smoother than those produced by uninterrupted gas-source MBE, but the differences are modest. In both samples substantial roughness occurs on a finer scale than generally deduced from optical measurements. We cannot, from our present measurements, decide why this is so. However, our results indicate that the cathodoluminescence intensity variations observed over distances of microns[8] probably represent not individual islands, but regions consisting of many islands, whose admixture changes as the probe is scanned. It is also possible that optical measurements do not probe the atomic scale roughness revealed by our technique. Our work may thus stimulate a more profound understanding of the correlation between the structural and optical properties of multilayered systems.

We now speculate on more general consequences of the approach outlined in this Letter. First, it makes possible the local quantification of the information content of lattice images. This should also allow the development of quantitative means for judging the success of a match between experimental and simulated images, a procedure fundamental to structure determination by lattice imaging. Second, by using pattern-recognition techniques, our approach allows sophisticated discrimination between noise and signal, and may thus help circumvent the pessimistic conclusions previously reached about the dominant effect of noise in lattice imaging, and its consequences for the detection of individual point defects.[15] Third, it presents a means for achieving near-atomic resolution spatially and chemically, thus opening the way for the study of chemical inhomogeneities and reactions on an atomic scale. These possibilities remain to be explored. Here we have presented results on the GaAs/AlGaAs system. It is clear, however, that a wide variety of interfaces and interfacial reactions, fundamental to modern materials, systems, and devices, can now be studied quantitatively at near-atomic resolution.

We acknowledge valuable discussions with D. S. Chemla, A. Y. Cho, J. S. Denker, L. C. Feldman, P. H. Fuoss, M. Grabow, L. Jackel, M. Panish, J. Shah, C. V. Shank, and C. A. Warwick, and expert technical assistance from J. A. Rentschler.

[1]P. M. Petroff, R. C. Miller, A. C. Gossard, and W. Wiegmann, Appl. Phys. Lett. **44**, 217 (1984).

[2]J. Singh, K. K. Bajaj, and S. Chaudhuri, Appl. Phys. Lett. **44**, 805 (1984).

[3]Y. Suzuki and H. Okamoto, J. Appl. Phys. **58**, 3456 (1985).

[4]M. Tanaka, H. Sakaki, and J. Yoshino, Jpn. J. Appl. Phys. Pt. 2 **25**, L155 (1986).

[5]R. Hull, K. W. Carey, and G. A. Reid, Mater. Res. Soc. Symp. Proc. **77**, 455 (1987).

[6]S. B. Ogale, A. Madhukar, F. Voillot, M. Thomsen, W. C. Tang, T. C. Lee, J. Y. Kim, and P. Chen. Phys. Rev. B **36**, 1662 (1987).

[7]S. Clarke and D. D. Vvedensky, J. Appl. Phys. **63**, 2273 (1988).

[8]D. Bimberg, J. Christen, T. Fukunaga, H. Nakashima, D. E. Mars, and J. N. Miller, J. Vac. Sci. Technol. B **5**, 1191 (1987).

[9]A. Ourmazd, W. T. Tsang, J. A. Rentschler, and D. W. Taylor, Appl. Phys. Lett. **50**, 1417 (1987).

[10]C. W. Tu, R. C. Miller, B. A. Wilson, P. M. Petroff, T. D. Harris, R. F. Kopf, S. K. Sputz, and M. G. Lamont, J. Cryst. Growth **81**, 159 (1987).

[11]A. Ourmazd and D. W. Taylor (to be published).

[12]More precisely, our analysis shows the interfacial unit cells to be (statistically) significantly different from those away from the interface. In these samples, we estimate the thickness difference between the centers of alternating GaAs and $Al_{0.37}Ga_{0.63}As$ regions to be less than 5 Å. Thus it is unlikely that the interface, which has a composition intermediate between those of the neighboring layers, has a significantly different thickness from the "bulk" areas. Preferential sample contamination near the interface is also unlikely to play an important role, because only changes that move the vector $\mathbf{R}^i$ along the plane containing the template vectors are important in our analysis. We thus conclude that genuine compositional change is the most likely cause for the observed difference between the interfacial unit cells and those in the "bulk."

[13]We note that the variations observed in the Al content near the interface are over and above those expected from the fluctuations in a random alloy. This is because such fluctuations have already contributed to the standard deviation σ of the normal distribution of "bulk" AlGaAs, and the differently colored interfacial unit cells differ by more than 3σ from the bulk unit cells.

[14]Tilt misalignment is currently the most serious limiting factor in all lattice-imaging techniques. Results on the extent to which our pattern-recognition approach can deal with tilt misalignments will be published elsewhere (Ref. 11). In the present work, when comparing different samples, we base our conclusions on many micrographs, obtained from different areas of several samples. In this way we attempt to ensure that our conclusions remain valid in spite of possible subtle differences between the imaging conditions used in different runs.

[15]J. M. Gibson and M. L. McDonald, Mater. Res. Soc. Symp. Proc. **82**, 109 (1987).

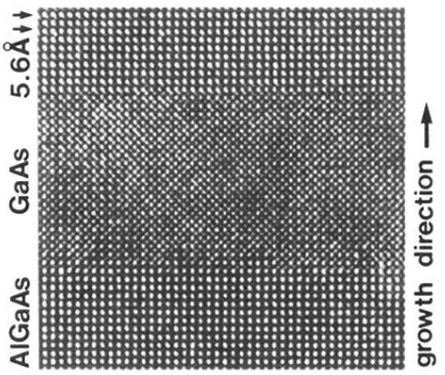

FIG. 1. Chemical lattice image of a GaAs/$Al_{0.37}Ga_{0.63}As$ quantum well produced after 2-min growth interruption at each interface. Careful inspection reveals interfacial regions have images intermediate between GaAs and $Al_{0.37}Ga_{0.63}As$.

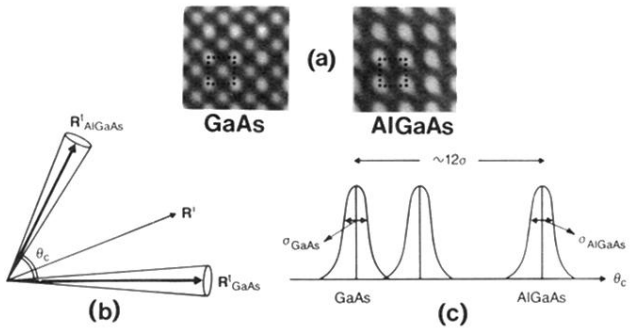

FIG. 2. (a) Averaged, noise-free images of GaAs and $Al_{0.37}Ga_{0.63}As$. The unit cells used as templates for pattern recognition are the dotted 2.8-Å squares. (b) Schematic representations of the template vectors $\mathbf{R}^i_{GaAs}$ and $\mathbf{R}^i_{AlGaAs}$, the distribution of $\mathbf{R}_{GaAs}$ and $\mathbf{R}_{AlGaAs}$ about them, and an interfacial vector $\mathbf{R}^i$. (c) Schematic representation of the distributions produced by the GaAs and $Al_{0.37}Ga_{0.63}As$ unit cells about their templates. Note that the angular position of $\mathbf{R}^i$ denotes the most likely composition only. The actual composition falls within a normal distribution about this point.

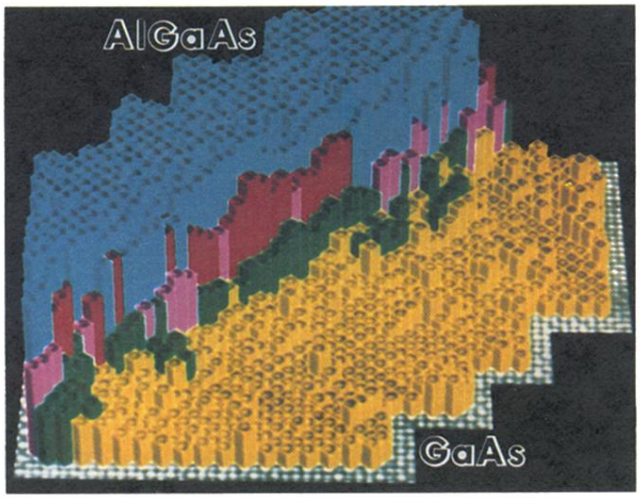

FIG. 3. Three-dimensional representation of the analyzed lattice image of $Al_{0.37}Ga_{0.63}As$ grown on GaAs after a 2-min interruption. The unit cells are 2.8-Å squares. The height of each cell represents the angular position of its vector **R** with respect to the template vectors, which are about 12σ apart. Yellow and blue mark those cells which fall within 3σ of GaAs and $Al_{0.37}Ga_{0.63}As$ templates, respectively. Green, magenta, and red represent 3σ bands centered about 3σ, 6σ, and 9σ points from GaAs. Outside the yellow and blue regions, the Al content of each unit cell is intermediate between GaAs and $Al_{0.37}Ga_{0.63}As$, with confidence levels given by normal statistics.

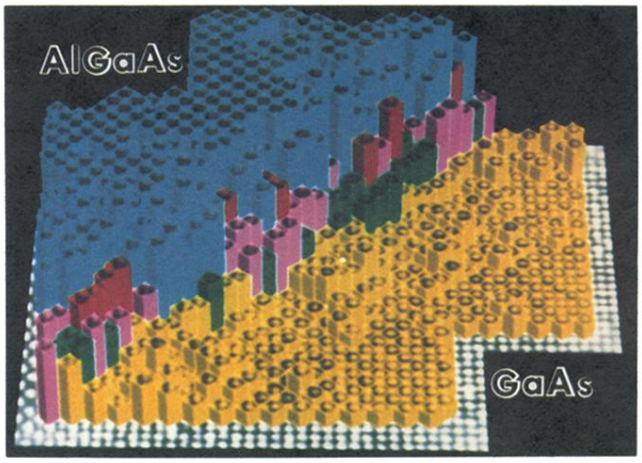

FIG. 4. Three-dimensional representation of the analyzed chemical image of $Al_{0.37}Ga_{0.63}As$ grown on GaAs without interruption. Color-coding and unit-cell size are the same as Fig. 3. Note the presence of small, disjointed clusters of color, indicating finer scale roughness.